Polyhedron 198 (2021) 115085

Contents lists available at ScienceDirect

Polyhedron

journal homepage: www.elsevier.com/locate/poly

Coordination and extraction properties of 1,2-bis(diphenylphosphoryl)-benzene toward *f*-block element nitrates: Structural, spectroscopic and DFT characterization of the complexes

Anna G. Matveeva [a,*], Oleg I. Artyushin [a], Margarita P. Pasechnik [a], Adam I. Stash [a], Anna V. Vologzhanina [a], Sergey V. Matveev [a], Ivan A. Godovikov [a], Rinat R. Aysin [a], Aleksandra A. Moiseeva [a], Alexander N. Turanov [b], Vasilii K. Karandashev [c], Valery K. Brel [a]

[a] Nesmeyanov Institute of Organoelement Compounds, Russian Academy of Sciences, ul. Vavilova 28, Moscow 119991, Russia
[b] Institute of Solid State Physics, Russian Academy of Sciences, Academician Osipyan str. 2, Chernogolovka 142432, Russia
[c] Institute of Microelectronics Technology Problems and High Purity Materials, Russian Academy of Sciences, Academician Osipyan str. 6, Chernogolovka 142432, Russia

ARTICLE INFO

Article history:
Received 20 November 2020
Accepted 1 February 2021
Available online 6 February 2021

Keywords:
1,2-bis(diphenylpsphoryl)benzene
f-element complexes
X-ray diffraction
Solution structure
Liquid extraction

ABSTRACT

Reaction of 1,2-bis(diphenylpsphoryl)benzene 1,2-$[Ph_2(O)P]_2C_6H_4$ (**L**) with *f*-element nitrates resulted in 1:1 and 1:2 complexes. The isolated complexes, namely, $[UO_2(\mathbf{L})(NO_3)_2]\cdot MeCN$ (**1**), $[UO_2(\mathbf{L})_2(NO_3)](NO_3)\cdot MeCN$ (**2**), $[Th(\mathbf{L})_2(NO_3)_3](NO_3)\cdot MeCN\cdot H_2O$ (**3**), $[La(\mathbf{L})_2(NO_3)_3]\cdot 0.5MeCN\cdot 1.5H_2O$ (**4**), and $[Lu(L)_2(NO_3)_2](NO_3)\cdot 2MeCN$ (**5**) have been characterized by elemental analysis and IR spectroscopy. The structures of complexes **1**, **2**, and **5** have been determined by single-crystal X-ray crystallography. Intraligand π-stacking and interligand C—H. . . π interaction have been observed in the crystalline complexes. The π-stacking and C—H. . . π interaction energy in two uranyl complexes **1** and **2** have been estimated from Bader's AIM theory calculations performed at the DFT level. Solution structure of all complexes has been investigated by IR and multinuclear (^1H, ^{13}C, and ^{31}P) NMR spectroscopy. The formation of 1:3 complexes with lanthanum nitrate (IR, ^{31}P NMR) has been examined. Preliminary extraction study of U(VI), Th(IV), and Ln(III) from 2 M HNO_3 into 1,2-dichloroethane have shown that ligand **L** recovers U(VI), Th(IV), and La(III) in the same extent as its tetraphosphoryl analog 1,2,4,5-$[Ph_2(O)P]_4C_6H_2$ (**L'**) but it recovers Eu(III), and Lu(III) by several times better than **L'**. Furthermore, an improved modified method for the synthesis of ligand **L** has been suggested.

1. Introduction

Phosphoryl-containing compounds are well-known and widely used ligands for complexation with lanthanides and other *f*-block elements [1–4]. They are extensively employed in liquid extraction for the recovery, preconcentration, and separation of these elements [5–7]. Polydentate neutral organophosphorus compounds show high efficiency in the recovery of actinides and lanthanides from nitric acid solutions; as a rule, it is much higher than that for monodentate analogs [8–12]. This feature favored to the development of coordination chemistry of phosphoryl-containing ligands, in particular, the studies of ability to coordinate ions of *f*-block elements [13,14].

Previously, we prepared a new neutral polyfunctional organophosphorus ligand 1,2,4,5-tetrakis(diphenylphosphoryl) benzene, which showed high efficiency in the recovery of *f*-block elements, in particular U(VI), Th(IV), and Ln(III), from nitric acid solutions [15]. It was of interest to study the extraction and coordination properties of a structural analog of this compound whose molecule contains only two rather than four $Ph_2P(O)$ groups: 1,2-bis(diphenylphosphoryl)benzene (**L**). This compound is known as efficient ligand for preparation of different complexes; however, its complexes with *f* element nitrates are not described.

In this paper, we report the modified synthesis of the bisphosphoryl-containing ligand **L** and its new complexes with uranyl (II), thorium(IV) and lanthanide(III) nitrates, the structural characterization of the complexes in the solid state (X-ray, IR) and in solution (IR, ^{31}P NMR, ^{13}C NMR, and ^1H NMR), and extraction studies toward the *f*-block elements. Furthermore, we report herein the results of AIM analysis (Bader's "Atoms in molecules" approach) for the π-stacking interactions in two uranyl complexes. The extraction ability of ligand **L** for the recovery of U(VI), Th(IV) and Ln(III) from nitric acid solution into 1,2-dichloroethane (DCE) in

* Corresponding author.
E-mail address: matveeva@ineos.ac.ru (A.G. Matveeva).

https://doi.org/10.1016/j.poly.2021.115085
0277-5387/

comparison with prototype, the 1,2,4,5-[$Ph_2P(O)]_4C_6H_2$ (**L'**), and structure analog 1,2-[$Ph_2P(O)CH_2]_2C_6H_4$ (**L''**), containing the same donor groups tethered to benzene platform *via* methylene linker, (Scheme 1) was evaluated.

2. Results and discussion

2.1. Synthesis of the ligand *L*

At present time, the literature reported a two-stage method for the preparation of bis(phosphine oxide) **L** using 1,2-dihalobenzene as an initial compound at the first stage. The 1,2-dihalobenzenes used were dichloro, dibromo, and diiodo derivatives, which were reacted in liquid ammonia with sodium diphenylphosphide. 1,2-Bis(diphenylphosphinyl)benzene obtained in a yield not higher 35% was next oxidized into bis(phosphine oxide) **L** [16]. Furthermore, a method was described where diphenylphosphinous acid was used as a phosphorus-containing reagent [17].

In this work, we prepared compound **L** by a modified procedure including the same stages as described previously [16] but using 1,2-difluorobenzene in tetrahydrofuran solution (instead of inconvenient liquid ammonia) followed by the oxidation of diphosphine with 30% H_2O_2 (Scheme 2).

This approach provided almost quantitative yields at both stages for both products: the diphosphine and the target ligand **L**. We used this approach previously in the synthesis of compound **L'** [15].

2.2. Synthesis and solid-state characterization of the complexes

The structure of complexes of ligand **L** with different metal salts was described in a series of works [18–26]. The studied complexes of ligand **L** with lanthanides were obtained using chloride [18] iodide [18] and PF_6^- [18] anions for La(III) and hexafluoroacetylacetonate for Eu(III) [19]. An effect of anions on the structure of the complexes was noted [18]. In all studied complexes [18–26], ligand **L** is coordinated in bidentate mode due to concerted orientation of phosphoryl groups. To our best knowledge, the complexes of bis(diphenylphosphoryl) ligand **L** with *f* element nitrates were not described.

Mononuclear complexes of ligand **L** with *f*-element nitrates–– $[UO_2(\mathbf{L})(NO_3)_2]\cdot MeCN$ (**1**), $[UO_2(\mathbf{L})_2(NO_3)](NO_3)\cdot MeCN$ (**2**), $[Th(\mathbf{L})_2(NO_3)_4]\cdot CH_3CN\cdot H_2O$ (**3**), $[La(\mathbf{L})_2(NO_3)_3]\cdot 0.5CH_3CN\cdot 1.5H_2O$ (**4**), $[Lu(\mathbf{L})_2(NO_3)_3]\cdot 2CH_3CN$ (**5**)— were prepared by the reaction of stoichiometric amounts of the ligand and the salts in MeCN. The composition and structures of the complexes in the solid state were studied using elemental analysis, and IR spectroscopy. The structures of the crystal complexes **1**, **2**, **5** were also elucidated by X-ray diffraction. All prepared complexes are readily soluble in CH_2Cl_2.

2.2.1. X-ray structures

According to the data of single crystal X-ray diffraction, the ditopic ligand acts as a bidentate-chelate one in both novel and previously characterized complexes. Thus, the uranium(VI) atom in complex **1** can interact also with two bidentate-chelate nitrate ions to form a hexagonal-bipyramidal UO_8 coordination polyhedron with uranyl oxygen atoms in the axial positions of the bipyramid (Figs. 1, 2). As a whole, the complex is neutral and has composition $[UO_2\mathbf{L}(NO_3)_2]$. Asymmetric unit of this compound contains the complex in a general position and an acetonitrile molecule.

In complex **2**, the uranium atom adopts a pentagonal bipyramidal coordination, with four oxygen atoms from two molecules of **L** and one oxygen atom of a nitrate anion in the equatorial plane (Figs. 3, 4).

Steric hindrances from two bulky ligands do not allow them to form a planar equatorial environment. The mean deviation of U1–O1–O2–O3–O4 atoms from a plane is equal to 0.12 Å (Fig. 4), as compared with 0.07(1) Å for U1 and all six oxygen atoms in the equatorial plane of **1** (Fig. 2). The elongation of thermal ellipsoids of oxygen atoms of **L** situated near the monodentate nitrate anion, the disorder of the coordinated anion, and the prominent deviation of the nitrate oxygen from the plane formed by the other atoms of uranium(VI) equatorial plane (0.26(1) and –0.65(1) Å) also demonstrate that there is not enough space in uranium(VI) equatorial plane even for the monocoordinated anion (Figs. 3, 4), and it should be rather labile. The unit cell of complex **2** contains the $[UO_2\mathbf{L}_2(NO_3)]^+$ cation, a highly disordered uncoordinated nitrate anion, and a disordered acetonitrile molecule.

As we mentioned above, the 1:2 complexes of lanthanides have been obtained before. Lanthanides in previously obtained $[La\mathbf{L}_2(H_2O)(EtOH)Cl_2]Cl\cdot EtOH$ [18] and $[Eu\mathbf{L}_2(HFAA)_2](HFAA)$ (HFAA is hexafluoroacetylacetonate) [19] and the novel $[Lu\mathbf{L}_2(NO_3)_2](NO_3)$ (**5**) complexes are eight-coordinated (Figs. 5, 6).

The lutetium(III) atom in the $[Lu\mathbf{L}_2(NO_3)_2]^+$ cation adopts square antiprism geometry with oxygen atoms from bidentate chelate ligand and NO_3^- in the each prism bases (Fig. 5). The third nitrate anion in complex **5** is uncoordinated; and the asymmetric unit of this complex contains a half of cation, a half of uncoordinated anion, and two independent acetonitrile molecules (each with half occupancy).

Selected interatomic distances in these complexes as well as in crystalline $\mathbf{L}\cdot CH_2Cl_2$ [22] are listed in Table 1. Uranyl group in both complexes is linear with O = U = O angles in $[UO_2\mathbf{L}(NO_3)_2]$, and $[UO_2\mathbf{L}_2(NO_3)]^+$ equal to 176.9(1) and 179.1(3)°, respectively, while r(U = O) are equal to 1.763(2) and 1.773(5) – 1.776(5) Å, respectively. The U – $O_{\mathbf{L}}$ distances in these complexes are nearly equal (these vary from 2.338(2) to 2.365(2) and from 2.338(5) to 2.386(4) Å), while the U – O_{NO3} distances for the chelate anion are longer than for the monodentate anion (2.515(2) – 2.518(2) as compared with 2.45(1) – 2.46(1) Å). Lanthanide contraction manifests itself as a shortening of Ln – $O_{\mathbf{L}}$ distances on passing from lanthanum (III) (2.448(4) – 2.522(4) Å [18]) to lutetium(III) (2.219(2) – 2.223(2) Å (Table 1)) complexes. The C—C and P—C bond distances within the **L** ligand remain almost unchanged upon coordination, with the P–C_{Bz} bonds being slightly longer than the P–C_{Ph} bonds. However, the P═O distances upon coordination become longer (Table 1).

Along with the P═O length change, the molecular conformation of the ligand significantly varies upon coordination. One of $Ph_2P(O)$

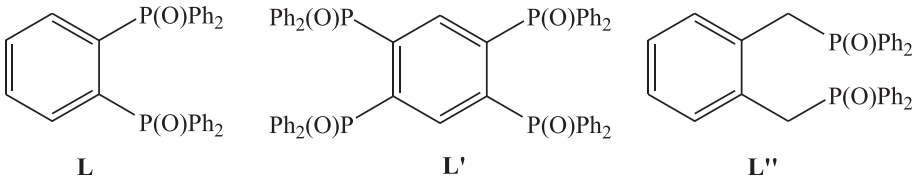

Scheme 1. Structure of bisphosphoryl ligand **L** and reference compounds **L'**, **L''**.

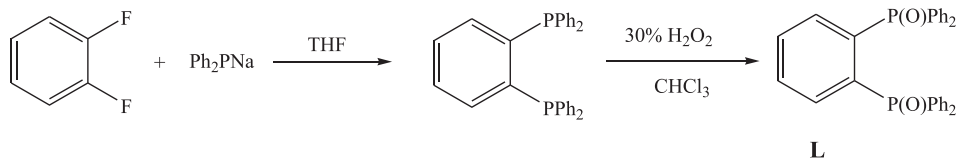

L

Scheme 2. Synthesis of the ligand **L**.

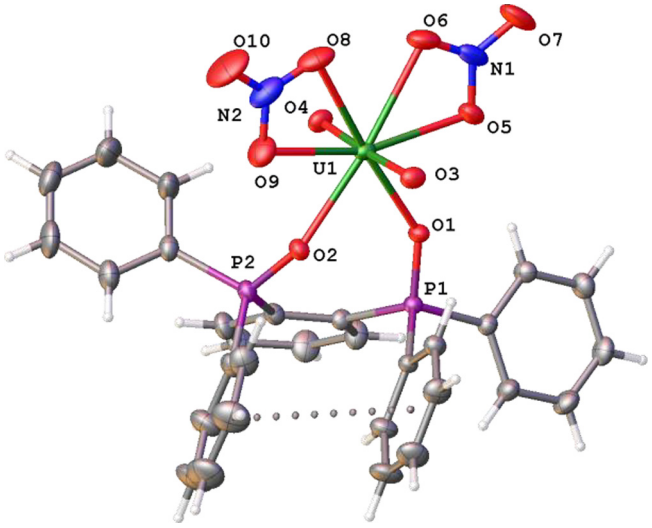

Fig. 1. Molecular view of the complex **1** in representation of atoms with thermal ellipsoids (given with 50% probability). Color code: C, grey; H, white; N, blue; O, red; U, green. The π-stacking interactions are depicted as dotted lines. (For interpretation of the references to colour in this figure legend, the reader is referred to the web version of this article.)

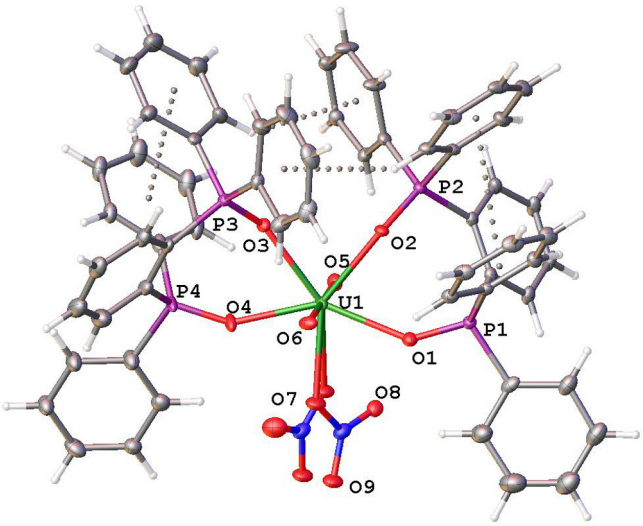

Fig. 3. Molecular view of the complex **2** in representation of atoms with thermal ellipsoids (given with 50% probability). Color code: C, grey; H, white; N, blue; O, red; U, green. The π-stacking and C—H… π intramolecular interactions are depicted as dotted lines. (For interpretation of the references to colour in this figure legend, the reader is referred to the web version of this article.)

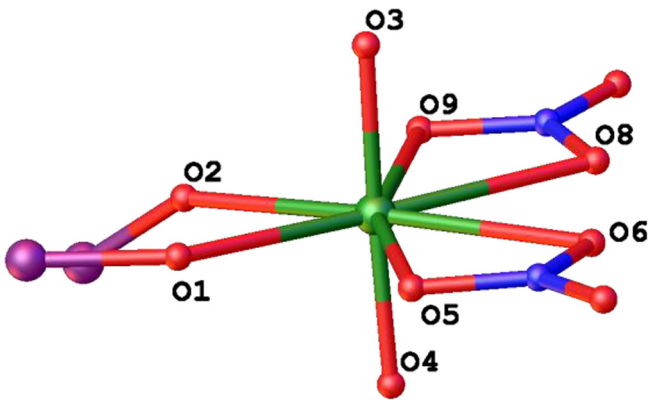

Fig. 2. The closest environment of U(VI) atom in complex **1**.

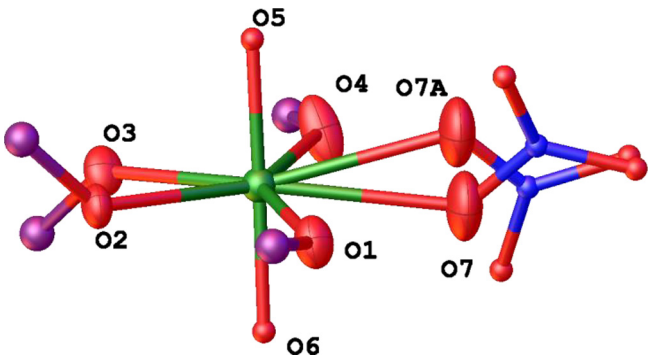

Fig. 4. The closest environment of U(VI) atom in cation of complex **2**. Oxygen atoms in the equatorial plane are depicted in thermal ellipsoids.

moieties rotates around the P-C_{Bz} bond by ~105° and the distance between the two P═O groups becomes ~0.3 Å shorter (Table 1). Fig. 7 shows the changes in the conformation of ligand **L** upon coordination.

Oxygen atoms of pure **L** are situated on the opposite sides of the plane formed by the benzene ring and two phosphorus atoms and on the same side for a coordinated ligand. As result, two of four phenyl rings in the coordinated ligand become nearly coplanar and take part in π…π stacking interactions (Fig. 7). Intercentroid distances between the rings vary from 3.711(5) to 3.877(1) Å. In the $[UO_2L_2(NO_3)]^+$ and $[LuL_2(NO_3)_2]^+$ cations, two intermolecular interligand C—H…π contacts between adjacent molecules of coordinated ligand can also be found with the distance from hydrogen atom to the center of phenyl rings as short as 2.996(4), 2.793(4) (Fig. 3), and 2.918(1) Å (Fig. 5). Thus, the π-stacking interaction between the two Ph substituents at two phosphorus atoms is observed in molecule(s) of coordinated ligand **L** for all crystalline complexes **1**, **2**, and **5**.

2.2.2. IR spectroscopy characterization

IR spectral data for ligand **L** and solid complexes **1**–**5** are presented in Table 2 (see also Figs. S1–S6).

The spectrum of complex **1** (Table 2, Fig. S2) corresponds to the structure established by X-ray diffraction.

According to X-ray diffraction data, the structures of complexes **2** and **1** differ mainly by the coordination of nitrate ions, one of which is coordinated in monodentate mode, while another anion

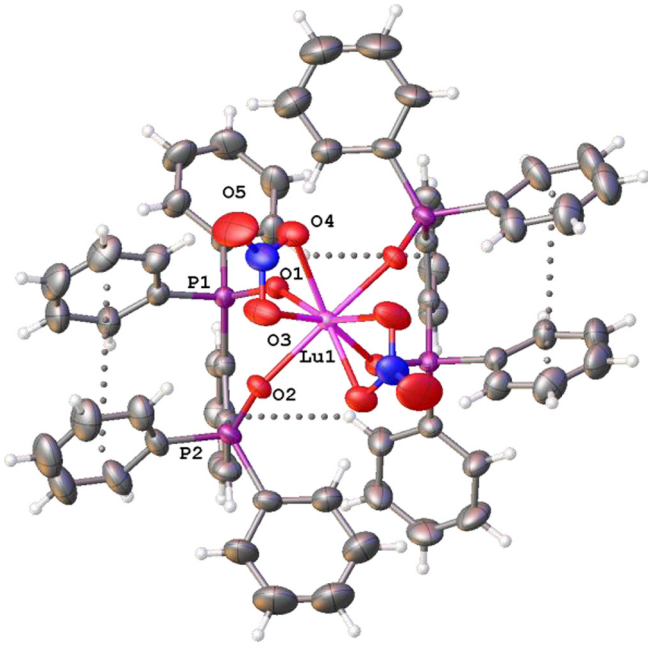

Fig. 5. Molecular view for cation of complex **5** in representation of atoms with thermal ellipsoids. Color code: C, grey; H, white; Lu, pink; N, blue; O, red. The π…π and C—H… π intramolecular interactions are depicted as dotted lines. (For interpretation of the references to colour in this figure legend, the reader is referred to the web version of this article.)

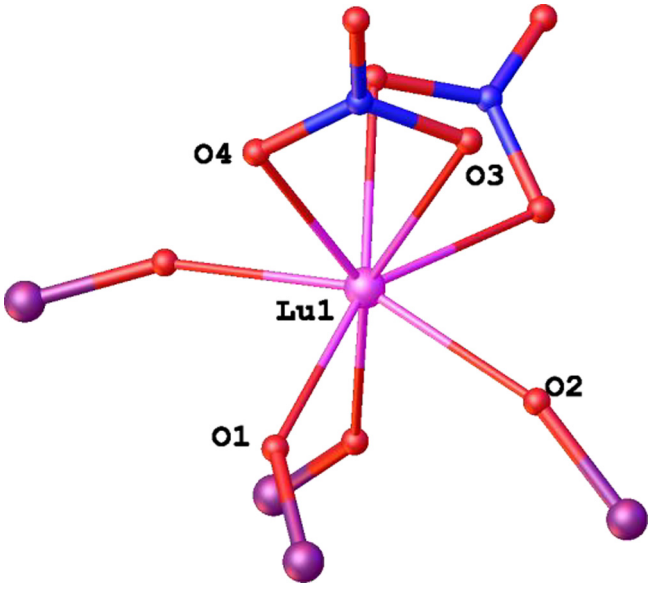

Fig. 6. The closest environment of Lu(III) atom in the cation of complex **5**.

is free. The IR spectrum of the complex **2** shows no bands typical for nitrate ion coordinated to uranyl ion in bidentate mode (see Table 2, Fig. S3), but displays the bands at 1296 and ~1020 cm^{-1}, which may be attributed to vibrations of nitrate ion coordinated in monodentate mode in accordance with the data for similar complexes [20,27]. The band at 1344 cm^{-1} belongs to vibration of free nitrate ion.

Complex **3** was obtained as a white powder, we failed to prepare crystals suitable for X-ray diffraction. The IR spectrum (Table 2, Fig. S4) shows a band of coordinated P═O groups of both ligand molecules at 1136 cm^{-1}. The IR spectrum shows certain features in the region of nitrate ions vibrations. The bands of nitrate ions coordinated in bidentate mode may be certainly revealed at 1512, 1288, and 1024 cm^{-1}, however, these bands have relatively low intensity and are broadened more than usually (Fig. S4). Although difference in mono- and bidentate nitrate coordination is uncertain, the coordination number (CN) twelve for thorium cation can be excluded in this case because of the bulky spatial structure of ligand **L** and its bidentate coordination. The structure $[Th(O,O\text{-}L)_2(O,O\text{-}NO_3)_2(O\text{-}NO_3)_2]$ with mono- and bidentate coordinated nitrate ions with CN 10 seems more likely. An alternative structure is $[Th(O,O\text{-}L)_2(O,O\text{-}NO_3)_3]^+(NO_3)^-$ (uncertain absorption at ~ 1350 cm^{-1}).

Complex **4** was obtained as a fine-crystalline powder; however, we failed to prepare crystals suitable for X-ray diffraction. IR spectrum (Table 2, Fig. S5) shows that both ligands are coordinated in bidentate mode: a strong band at 1178 cm^{-1} corresponds to ν (P═O) vibrations. Nitrate ions are also coordinated, but it is not excluded that one or two of them are bound in monodentate mode, because the maxima of $\nu(NO_3)$ bands were revealed at 1317 and 1030 cm^{-1}, but each band has a low-frequency shoulder (high-frequency band $\nu(NO_3)$ is not determined because of Nujol absorption). Therefore, CN of lanthanum cation is 9 or 8. Let us note that the CN of metal in the crystalline complexes of ligand **L** with lanthanum chloride [18] and the second group metal nitrates (Mg, Ca, Ba, Sr [20]) was not larger than 8 according to X-ray diffraction.

The spectrum of complex **5** (Table 2, Fig. S6) corresponds to the structure established by X-ray diffraction.

2.3. Solution-state characterization of the complexes

The structure of the complexes in CD_2Cl_2 solutions was studied by IR and multinuclear NMR spectroscopy. The selected parameters of IR and $^{31}P\{^1H\}$, $^{13}C\{^1H\}$ NMR spectra for the complexes **1**–**5** in comparison with the data for the free ligand **L** are given in Table 3 (see also Figs. S7–S13, and S14–S31).

The coordination of the P═O groups can be reliably determined from the NMR spectra of compounds **1**–**5**. The signals of the phosphorus nuclei exhibit expected downfield shifts by 5–18 ppm (Table 3) close to those for the known complexes [18]. The signals of carbon nuclei also show expected shifts. The signals δ_C(C-1,2) and δ_C(C-1′) in $^{13}C\{^1H\}$ NMR spectra are shifted upfield by 1–3 and ~5–8 ppm, respectively (Table 3). The signals of other carbon atoms in the benzene platform are shifted downfield by ~2 ppm. The signals of the phenyl substituents δ_C(C-4′) and δ_C(C-2′,6′) exhibit slightly larger downfield shifts than the δ_C(C-3′,5′) signals. The signals of ^1H NMR spectra are broadened for complexes **4**, **5** and considerably broadened for complexes **1**, **2**.

The IR spectrum of complex **1** solution (Fig. S8) is almost the same as the spectrum of crystalline sample (Fig. S2), this fact implies that the structure of the complex in solution is the same as in crystal. However, the $^{31}P\{^1H\}$ NMR spectrum displays two signals at 49.0 and 46.4 ppm with integral intensity ratio of ~ 1:5 (Fig. S17). The $^{13}C\{^1H\}$ NMR spectrum also shows two sets of signals of different intensity (Fig. S19). The chemical shifts in both spectra differ considerably from the signals of free ligand (Table 3) and unambiguously indicate the bidentate coordination of ligand molecule. We can suppose that we observe an equilibrium in NMR time scale of two isomers of complex $[UO_2(O,O\text{-}\mathbf{L})(O,O\text{-}NO_3)_2]^0$, where both nitrate ions are coordinated in bidentate mode (δ_P = 46.4 ppm), and $[UO_2(O,O\text{-}\mathbf{L})(O,O\text{-}NO_3)(O\text{-}NO_3]^0$, where one nitrate ion is coordinated in monodentate mode (δ_P = 49.0 ppm). This assumption agrees well with quantum chemical calculations on the existence of two such isomers (*vide infra*). Along with the noted species in solution, the equilibrium may include a contact ion pair (CIP) of complex $[UO_2(O,O\text{-}\mathbf{L})(O,O\text{-}NO_3)]^+\cdot(NO_3)^-$ (the sig-

Table 1
Selected interatomic distances (Å) in compounds **L**, **1**, **2**, and **5**.

Parameter	**L** [22]	**1**	**2**	**5**
Metal atom		U(VI)	U(VI)	Lu(III)
U = O		1.763(2)	1.773(5) – 1.776(5)	
M – O_L		2.338(2) – 2.365(2)	2.338(5) – 2.386(4)	2.219(2)–2.223(2)
M – O_{NO3}		2.515(2) – 2.518(2)	2.45(1) – 2.46(1)	2.366(2) – 2.412(2)
P=O	1.484(2) – 1.485(2)	1.497(2) – 1.504(2)	1.494(4) – 1.513(4)	1.495(2) – 1.503(2)
P – C_{Ph}	1.7999(3) – 1.815(3)	1.787(3) – 1.796(3)	1.778(9) – 1.808(5)	1.788(2) – 1.796(3)
P – C_{Bz}	1.824(3) – 1.838(3)	1.807(3) – 1.822(3)	1.819(6) – 1.829(6)	1.817(2) – 1.818(2)
Cg…Cg[a]		3.846(2)	3.711(5) – 3.733(5)	3.877(1)
P=O…O=P	2.977(4)	2.681(3)	2.716(6) – 2.738(8)	2.715(2)

[a] The distance between the centers of two parallel Ph rings in the ligand **L**.

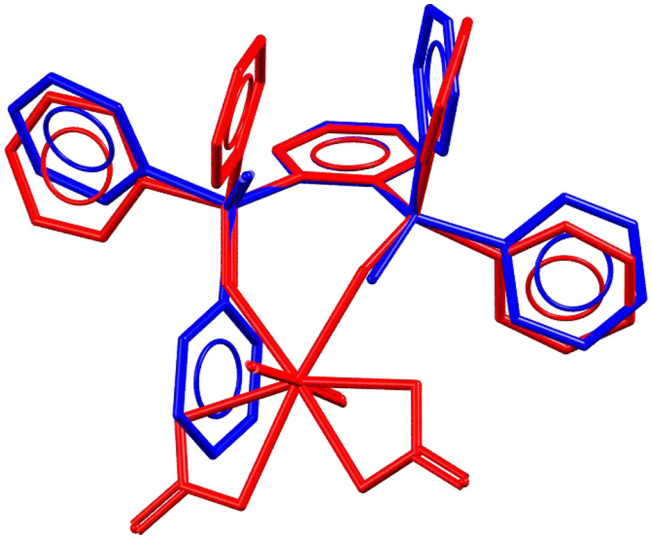

Fig. 7. Conformation of uncoordinated **L** (blue) as compared with the coordinated molecules in complex **1** [UO_2**L**$(NO_3)_2$] (red). Overlaid atoms are six carbon atoms of the benzene ring, and two phosphorus atoms. (For interpretation of the references to colour in this figure legend, the reader is referred to the web version of this article.)

nal at 49.0 is broadened). It should be noted that the presence of two (and more) signals of coordinated P=O groups in $^{31}P\{^1H\}$ NMR spectra for the complexes of phosphoryl-containing ligands is infrequent and the observed equilibrium for certain compounds is explained by change in anion coordination (monodentate, bidentate, free anion) in the species with different chemical shifts [18,20,26,28]. The ^1H NMR spectrum of complex **1** is considerably broadened (Fig. S18), which indicates the presence of dynamic processes in solution.

According to the data of IR spectroscopy (Table 3), the structure of biligand uranyl complex in solution is similar to the structure in crystal. The $^{31}P\{^1H\}$ NMR spectrum of solution shows two narrow singlets at 46.5 and 46.3 ppm with integral intensity ratio of ~ 5::1 (Fig. S20). The $^{13}C\{^1H\}$ NMR spectrum also exhibits two sets of signals of different intensity (Fig. S21). The slight difference in δ_P values (0.2 ppm) allows us to suppose that the monodentate coordination of nitrate ions in both species retains, while the observed difference can be explained by the existence of equilibrium of isomers of different structure (see below, Section 2.4). The ^1H NMR spectrum is considerably broadened, which indicates the occurrence of dynamic processes. The equilibrium includes ionic complexes $[UO_2(O,O\text{-}\mathbf{L})_2(O\text{-}NO_3)]^+\cdot(NO_3)^-$ and $[UO_2(O,O\text{-}\mathbf{L}^*)_2(O\text{-}NO_3)]^+\cdot(NO_3)^-$ ($\mathbf{L}^*$ are ligand molecules that differ by the presence of additional intramolecular interactions), the coordination number of uranyl cation in both species is 5.

Table 2
Selected IR (ν, cm^{-1}) spectroscopic data for ligand **L** and its complexes with *f*-element nitrates **1**–**5** in crystalline and solid state.

Compound	ν(P=O)	ν(NO_3)
L	1203vs	–
1[a]	1160vs, 1146sh	1517vs, 1490sh, 1288s 1273sh, 1264sh, 1027 m
2[a]	1142vs, 1149sh	1470m br [b], 1344m, 1296m, ~1020w
3	1136s	1512m, 1288m br, 1023w
4	1178vs	* [c], 1317s, 1295sh, 1036w, 1031sh
5 [a]	1167s, 1145s	~1500m, 1340m, 1305m, 1027w

[a]Crystalline compound.
[b]In the spectrum of sample as a KBr pellet.
[c]Expected band of ν(NO_3) is obscured by the Nujol absorption.

The IR spectrum of complex **3** displays a split band of coordinated P=O groups with maxima at 1143 an 1136 cm^{-1} (Fig. S10). The bands ν(NO_3) appear at 1519 and 1288 cm^{-1} and correspond to NO_3 groups coordinated in bidentate mode, however, these bands have a complex form and unusual broadening. The band of free nitrate ion is observed at 1352 cm^{-1}. One can suppose that coordination polyhedron includes nitrate ions coordinated in bi- and monodentate mode. The $^{31}P\{^1H\}$ and $^{13}C\{^1H\}$ NMR spectra show one set of signals indicating the bidentate coordination of both ligand molecules (Fig. S23, S25). The signals in ^1H NMR are resolved and show fine structure (Fig. S24). One can assume that complex **3** exists in solution as a solvent-separated ion pair (SSIP) $[Th(O,O\text{-}\mathbf{L})_2(O,O\text{-}NO_3)_2(O\text{-}NO_3)]^+\cdot(NO_3)^-$, the CN of thorium is 9.

The IR spectrum of solution of complex **4**, as distinct from the spectrum of solid complex, exhibits a weak absorption at 1204 cm^{-1} whose position coincides with that of ν(P=O) band of free phosphoryl group. An intense band of coordinated P=O groups is observed at 1180 cm^{-1} with a weak shoulder at ~ 1175 cm^{-1} (Fig. S11). The broad unresolved band at ~ 1460 and the shoulder at 1300 cm^{-1} should be assigned to vibrations of nitrate ions coordinated in bidentate mode, while the band at 1324 cm^{-1} refers to vibrations of monodentate nitrate ions. There is no band of free nitrate ions (Fig. S11). The $^{31}P\{^1H\}$ and $^{13}C\{^1H\}$ NMR spectra display one set of signals indicating the bidentate coordination of both ligand molecules (Fig. S26, S28). However, the signals in ^1H NMR spectrum are broadened (Fig. S27). One can suppose that complex **4** in solution exists in equilibrium as a contact ion pair (CIP) $[La(O,O\text{-}\mathbf{L})_2(O,O\text{-}NO_3)_2]^+\cdot(NO_3)^-$, neutral complex $[La(O,O\text{-}\mathbf{L})_2(O,O\text{-}NO_3)(O\text{-}NO_3)_2]^0$, and a small portion of monoligand complex $[La(O,O\text{-}\mathbf{L})(O,O\text{-}NO_3)_3]^0$ whose emergence is accompanied by the presence in solution of small amount of free ligand. In contrast to IR time scale, these equilibria refer to fast processes in the NMR time scale. Lanthanum cation CN is 8 in the all considered structures.

Table 3
Selected IR (ν, cm^{-1}), $^{31}P\{^1H\}$ and $^{13}C\{^1H\}$ NMR (δ, ppm) spectroscopic data for the ligand **L** and its complexes **1**–**5** with *f*-element nitrates in CD_2Cl_2 (0.01 M) at 25 °C.

Compound	ν(P═O)	δ_P ($W_{½}$)[a]	δ_C(C-1,2)	δ_C(C-1′)	δ_C(C-3,6)	δ_C(C-4,5)	ν(NO_3) coord	$\nu_E(NO_3)$ free
L	1204s	30.7 (0.01)	136.70 dd	134.03 d	135.86t	130.87 dt		
1	1165s, 1146sh	49.0 (0.24), 46.4 (0.07) [b]	134.19 dd[c]	128.00 d [c]	137.47t [c]	133.00 dt [c]	1525vs, 1495sh, 1288sh, 1270s, 1028w	–
2	1147s	46.5 (0.05), 46.3 (0.02) [d]	134.04 dd[c]	127.86 d [c]	137.57 t [c]	133.03 dt br	1470sh, 1387m, 1296m	1354m
3	1143sh,1136vs	44.9 (0.01)	133.21 dd	126.43 d	137.84t	133.13 dt	1519s, 1288s	1352m
4	1204sh,1180vs, 1175sh	35.4 (0.05)	135.85 dd	129.44 d	136.84t	131.50 dt	~1460sh br, 1324m, 1300sh	–
5	1204sh,1174vs, 1147sh	41.9 (0.05)	134.22 dd	127.29 d	137.86t	133.17 dt	1524m br, 1503m br, 1299s	1352s

[a]The band width at half-height (in ppm).
[b]Integral intensity ratio is ~*1*:*5*.
[c]Minor signals (see the corresponding figures in ESI).
[d]Integral intensity ratio is ~*5*:*1*.

The IR spectrum of solution of complex **5** shows rather distinct ν(P═O) band of free P═O group at 1204 cm^{-1} along with the strong band of coordinated P═O groups at 1174 cm^{-1} with shoulder at 1147 cm^{-1} (Table 3). The spectrum displays rather strong band of free nitrate ions at 1352 cm^{-1}. The spectrum also exhibits the broad split bands of NO_3 groups at 1524 and 1503 cm^{-1} and a band at 1299 cm^{-1} (Fig. S12). This spectral pattern may correspond to the presence in solution of several complex species with free and coordinated mono- and bidentate nitrate ions. The $^{31}P\{^1H\}$ and $^{13}C\{^1H\}$ NMR spectra show one set of signals indicating the bidentate coordination mode of both ligand molecules (Table 3, Fig. S29, S31). The signals in ^1H NMR spectrum are broadened (Fig. S30). The $^{31}P\{^1H\}$ NMR spectrum changes upon consecutive cooling to 200 K (Fig. 8). One narrow singlet is observed at 291 K, it is broadened and slightly shifted upon further cooling; the spectrum shows two very broad resonances at 220 K and two singlets at 45.2 and 39.8 ppm of equal intensity at 200 K.

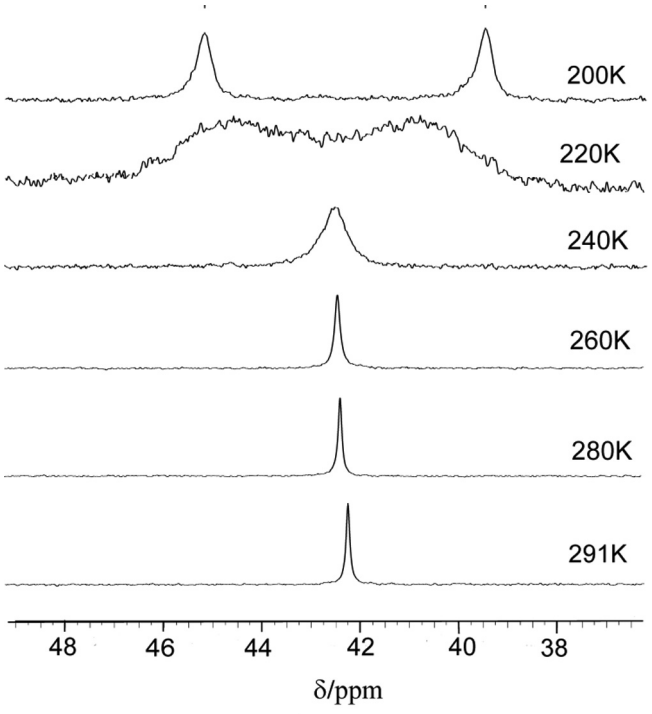

Fig. 8. Variable temperature $^{31}P\{^1H\}$ NMR spectra (121.49 MHz) of complex **5** in CD_2Cl_2.

Both values can be related to the chemical shifts of coordinated phosphoryl groups in ionic complexes of lutetium with different coordination of nitrate ions that vary "efficient charge" of cation and the corresponding shielding of phosphorus atom [20,28]. Variable temperature NMR spectroscopic study shows the existence of two isomers of complex **5**. One can assume that solution contains $[Lu(O,O\text{-}\mathbf{L})_2(O,O\text{-}NO_3)]^{2+}\cdot 2(NO_3)^-$, ($\delta_P$ = 45.2 ppm) and $[Lu(O,O\text{-}\mathbf{L})_2(O,O\text{-}NO_3)_2]^+\cdot(NO_3)^-$, ($\delta_P$ = 39.8 ppm) species in equilibrium at 200. K. While the main species is $[Lu(O,O\text{-}\mathbf{L})_2(O,O\text{-}NO_3)(O\text{-}NO_3)]^+\cdot(NO_3)^-$ (δ_P = 41.9 ppm) at 291 K. Along with these equilibria at ambient temperature, the equilibrium also includes monoligand complex $[Lu(O,O\text{-}\mathbf{L})(O,O\text{-}NO_3)_3]^0$ and the corresponding amount of free ligand whose band is detected in IR spectrum. These equilibria at ambient temperature are fast in the NMR time scale. The CN of lutetium cation in the noted species is 6, 7, or 8.

By the example of reaction of ligand **L** with $La(NO_3)_3$, we examined the possibility to form complexes of composition La:**L** = 1:3. The addition of equimolar amount of **L** to complex **4**, IR spectrum displays the emergence of absorption at 1350 cm^{-1}, which indicates the appearance of free NO_3 groups (Fig. S13). The remaining spectrum is close to the spectrum of complex **4**, it also shows a weak absorption of free P═O groups at 1204 cm^{-1}. The $^{31}P\{^1H\}$ NMR spectrum of solution displays singlets at 36.9 ($W_{½}$ = 0.5), 35.2 ($W_{½}$ = 1.2), and 30.6 ($W_{½}$ = 0.02) ppm with integral intensity ratio of ~1:2.4:0.01 (Fig. S32). One can suppose that equilibrium in solution involves trisligand complexes $[La(O,O\text{-}\mathbf{L})_3(O,O\text{-}NO_3)]^{2+}\cdot(NO_3)^-$ (δ_P = 36.9 ppm) and $[La(O,O\text{-}\mathbf{L})_3(O\text{-}NO_3)_2]^+\cdot(NO_3)^-$ (δ_P = 35.2-ppm), as well as a small amount of bisligand complexes $[La(O,O\text{-}\mathbf{L})_2(O,O\text{-}NO_3)_2]^+\cdot(NO_3)^-$ and $[La(O,O\text{-}\mathbf{L})_2(O,O\text{-}NO_3)(O\text{-}NO_3)_2]^0$ (δ_P = 35.2–35.4 ppm), which is accompanied by the corresponding amount of the free ligand (δ_P = 30.6 ppm).

Thus, the strong bidentate coordination of ligand retains in the complexes **1**–**5** in CD_2Cl_2 solutions. The coordination of nitrate ions varies from bi- to monodentate and to free nitrate ions within CIP or SSIP. The cation of large radius La(III) can form trisligand cationic complexes in solution.

*2.4. DFT study and QTAIM analysis for complexes **1** and **2***

The DFT analysis for monoligand complex $[UO_2\mathbf{L}(NO_3)_2]$ and cation of bisligand complex $[UO_2\mathbf{L}_2(NO_3)]^+$ was performed at the PBE/6-311G**, MWB60 level. All found isomers include the bidentate coordination of ligand molecules and intraligand πstacking.

The DFT results for monoligand complex $[UO_2\mathbf{L}(NO_3)_2]$ revealed two isomers: **1a** (X-ray geometry) and **1b**. In the structure **1a**, both nitrate ions are coordinated in bidentate mode (Fig. S33a, b), while the structure **1b** includes one of nitrate ions coordinated in mon-

odentate mode (Fig. S34a, b). The πstacking energy in both isomers is the same, 1.1 kcal·mol^{-1} (Табл. S1). Complex **1a** is favored over **1b** by 6.15 kcal·mol^{-1} (Table 4).

For cation of bisligand complex $[UO_2\mathbf{L_2}(NO_3)]^+$, we revealed four isomers: two isomers **2a** (X-ray geometry) (Fig. S35a, b) and **2b** (Fig. S36a, b) with monodentate nitrate coordination, and two isomers **2c** (Fig. S37) and **2d** (Fig. S38) with bidentate nitrate coordination. The isomers of each pair **2a**, **2b** and **2c**, **2d** differ from each other by the spatial arrangement of the ligand molecules. Let us note that in the case of isomers **2a** and **2c**, we observed the formation of two πstacking and two CH…π interactions in both ligand moieties, whereas there are no CH…π contacts for isomers **2b** and **2d**. In all studied cases, π-stacking and additional CH…π contacts characterize two bond paths (Fig. 9a, b) (except for isomer **2d** containing one bond path).

The energy of π-stacking and CH…π contacts for the all isomers are juxtaposed in Table S1. The obtained π-stacking interaction energy values for isomers of 1.2–2.4 kcal mol^{-1} (Table S1) are close to those for intramolecular π-stacking in a Co(III) complex [30] of about 1–3 kcal mol^{-1} and to those for intramolecular π-stacking interactions in UO_2(II) complexes [31] of about 2.0–2.3 kcal mol^{-1}. Isomers with monodentate coordination of nitrate ion **2a**, **2b** are slightly more preferable than isomers **2c**, **2d** with nitrate ion coordinated in bidentate mode approximately by 1.3–2.3 kcal mol^{-1}, which also indicates the possibility of their simultaneous presence in solution.

The obtained results (Table 4) agree well with the assumption that solutions of complexes **1** and **2** contain equilibrium mixture of species that differ considerably in ΔG^o_{298} and δ_P values for complex **1** and slightly differ in the case of complex **2**.

Let us note that the calculated interatomic distances and angles in structures **1a** (Fig. S33a) and **2a** (Fig. S35a) generally agree with values found in crystalline complexes **1** and **2** by X-ray diffraction. One π-stacking and two π-stacking and two CH…π interactions according to X-ray diffraction data are observed in crystalline complexes **1** and **2**, respectively (see above, Figs. 1, 3).

2.5. Solvent extraction of f-block elements

To compare the efficiency and selectivity of the studied ligand **L** as well as its tetraphosphoryl prototype **L'** [15] and extractant **L"** [29] we studied the distribution ratios (D = $[M]_{org}/[M]_{aq}$) for uranium(VI), thorium(IV), and several lanthanides(III) (Figs. 10, 11).

Fig. 10 shows that both ligands **L** and **L'** almost similarly recover thorium, but ligand **L** extracts uranium slightly better. Compound **L"**, where $Ph_2P(O)$ groups are bound to benzene platform *via* methylene linkers, recovers uranium much worse and does not recover thorium. This compound also does not recover lanthanides (D_{Ln} < 0.003).

Extraction efficiency and selectivity is known to be dependent in complicated manner on numerous factors, including the strength and structure of extracted complexes, hydrophilicity/lipophilicity balance of a ligand and its complexes.

In the case of close structure and the same coordination type of ligands, we can analyze extraction data in the first approximation by the comparison of composition and structure of extracted and individual (model) complexes in solution. Let us note that the lipophilicity of ligands **L** and **L'** is close according to preliminary data (the data will be reported elsewhere).

The structure of individual complexes of ligand **L'** is not studied yet, but the composition of extracted species is known [15]. It was found that species extracted into chloroform have metal:ligand composition of 1:1.5 for U(VI) and 1:2 for Th(IV). One can suppose that compound **L** will extract these actinides most likely as species

Table 4
Relative energies of isomers of complex $[UO_2\mathbf{L}(NO_3)_2]$ and isomers of complex cation $[UO_2\mathbf{L_2}(NO_3)]^+$.

Isomer	E_{tot}, a.u.	ΔE_{tot}, kcal/mol	G^o_{298}, a.u.	ΔG^o_{298}, kcal/mol
1a (X-ray geometry) η^2-NO_3, η^2-NO_3	−3177.082162	0.00	−3176.633075	0.00
1b η^1-NO_3, η^2-NO_3	−3177.071747	6.54	−3176.623274	6.15
2a[a] (X-ray geometry) η^1-NO_3	−4886.162741	0.00	−4885.279905	0.00
2b η^1-NO_3	−4886.164879	−1.56	−4885.280910	−0.63
2c[a] η^2-NO_3	−4886.160258	1.34	−4885.277871	1.28
2d η^2-NO_3	−4886.162535	+0.13	−4885.277201	1.70

[a] CH…π contacts are present.

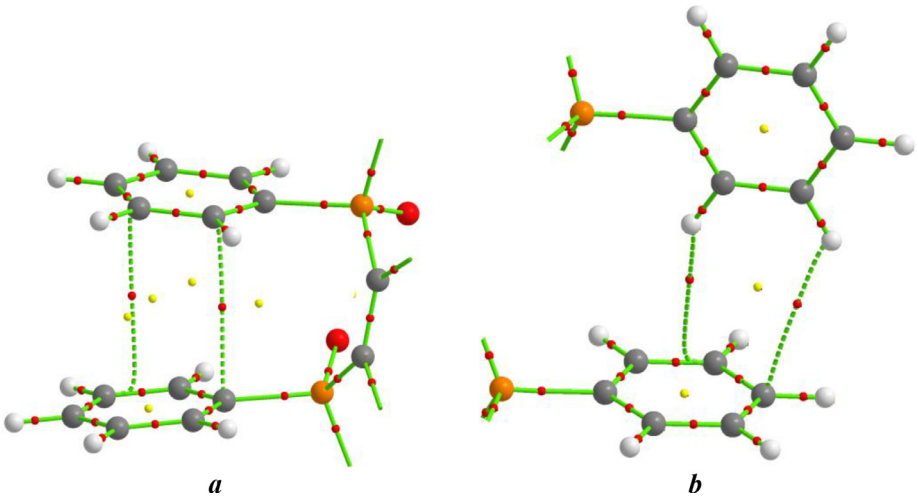

Fig. 9. The typical fragments of molecular graph exhibit the π-stacking (***a***) and CH…π contacts (***b***) in the isomers of complexes **1** and **2**. Color codes for the atoms: red (O), orange (P), grey (C), white (H). The π-stacking and CH…π contact bond paths are shown as green dotted lines; BCPs (3;−1) are red. (For interpretation of the references to colour in this figure legend, the reader is referred to the web version of this article.)

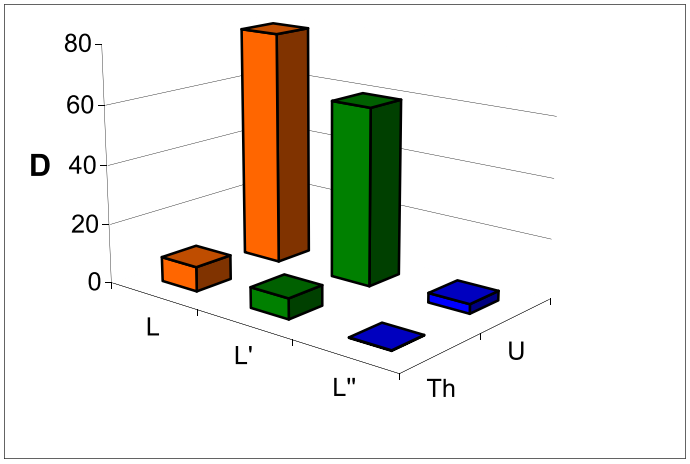

Fig. 10. Comparison of the distribution ratios of U(VI) and Th(IV) for the extraction from 2 M HNO_3 with 0.0001 M solutions of compounds **L** [this work], **L'** [15] and 0.01 M solution of compound **L"** [29] in DCE; the initial concentration of uranyl and thorium nitrates in the aqueous phase is $2 \cdot 10^{-6}$ M. (Color online.)

of the same composition as **L'**, both ligands seem to exhibit the same denticity. Then one can expect that D_U and D_{Th} values will be close for both extractants (as it is seen in Fig. 10).

Neutral complexes are known to be more lipophilic and better extracted into organic solvent than ionic ones. This feature seems to be one of the reasons of better recovery of U(VI) with both extractants (Fig. 10) because U(VI) is extracted as a mixture of neutral monoligand and ionic bisligand complexes in contrast to Th (IV).

Fig. 11 shows that recovery efficiency for ligands **L** and **L'** in the series of studied Ln(III) varies in different manner. It was found that compound **L'** extracts Ln(III) as species with metal:ligand composition of 1:2 [15]. Decrease of D_{Ln} in the series La–Lu is reasonably explained by the decrease of cation radius for Ln, which results in expulsion of nitrate ion and increase in the content of ionic complexes if composition and coordination mode for ligand **L'** retains.

Ligand **L**, as distinct from ligand **L'**, forms in solution ionic complex with metal:ligand ratio of 1:3 (this work), which leads to increase in the content of ionic less extracted species. Since the strong chelate coordination of compound **L** retains in the all studied complexes, the composition of extracted species will approach to 1:2 when Ln radius decreases, while recovery efficiency will increase until further drop of Ln cation radius leads to the expulsion of the next nitrate ion and the growth of the content of poorly extracted ionic pairs of complexes in solution. The aggregate action of these factors leads to considerable difference in the profile of D_{Ln} variations for the series of the studied lanthanides for **L** and **L'** (Fig. 11).

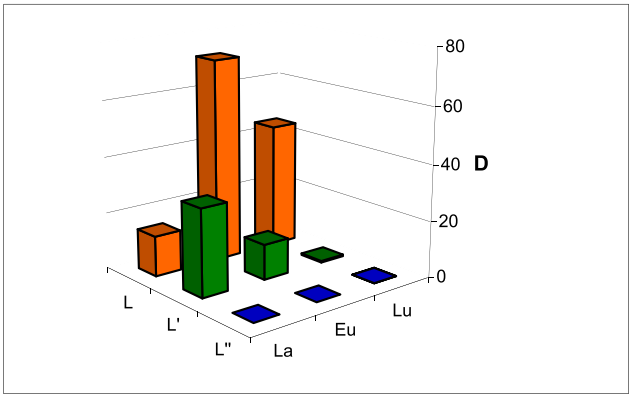

Fig. 11. Comparison of the distribution ratios of La(III), Eu(III), and Lu(III) for the extraction from 2 M HNO_3 solution with 0.02 M solutions of compounds **L**, **L"**, and 0.01 M solution of compound **L'** [15] in DCE; the initial concentration of lanthanide nitrates in the aqueous phase is $2 \cdot 10^{-6}$ M.

In summary, the efficiency of La(III) recovery with ligand **L'** is almost twice as high as with ligand **L**. The efficiency of Eu(III) and Lu(III) recovery with ligand **L** is higher than for its tetraphosphoryl analog by 9 and 80 times, respectively. Extraction selectivity also differs considerably. Separation factor for La and Eu ($S_{La/Eu} = D_{La}/D_{Eu}$) for ligand **L** is twice as high as for ligand **L'**.

The study of extraction properties of ligand **L** and the structure of complexes of ligand **L'** is in progress.

Taking into account the obtained data, we should emphasize that bisphosphoryl ligand **L** is more convenient and promising candidate for the further study of *f*-element extraction than tetraphosphoryl compound **L'**.

3. Conclusion

Coordination properties of the neutral organophosphorus ligand L toward *f*-block element nitrates were examined. The bisligand complexes of **L** with U(VI), Th(IV), La(III) and Lu(III) nitrates were studied in the solid state (X-ray, IR) and solution (IR, ^{31}P NMR, ^{13}C NMR, and ^{1}H NMR). The bulky bisphosphoryl ligand **L** exhibits constant PO,PO-denticity in all studied complexes both in solid state and solutions. Nitrate ions show variable denticity. We revealed bi- and monodentate coordination of nitrate ions and even the presence of free uncoordinated ions. The extraction experiments revealed that the studied bisphosphoryl ligand 1,2-$[Ph_2P(O)]_2C_6H_4$ (**L**) recovers Th(IV) and U(VI) by the same extent as its tetraphosphoryl prototype 1,2,4,5-$[Ph_2P(O)]_4C_6H_2$ (**L'**) and extracts Eu(III) and Lu(III) considerably better than **L'**. Both ligands **L** and **L'** are considerably superior over the bisphosphoryl ligand with methylene linkers between the phosphoryl group and the benzene ring 1,2-$[Ph_2P(O)CH_2]_2C_6H_4$ (**L"**) in terms of the recovery efficiency of *f*-block elements from nitric acid solutions in DCE.

4. Experimental

4.1. General

Solvents were purified and dried using standard procedures [32]. Deuterated solvents CD_2Cl_2 (99.9% D, Cambridge Isotope Lab-

oratories, Inc.) and $CDCl_3$ (99.8% D, Sigma–Aldrich) were used as received. Multinuclear ^1H, ^{13}C, and ^{31}P. NMR spectra were recorded on a Bruker Avance 400 spectrometer (operating at 400.23, 100.61, and 161.98 MHz, respectively), and a Bruker Avance 500 instrument (operating at 500.15, 125.75 and 202.46 MHz, respectively) at ambient temperature using CD_2Cl_2 (c = 0.01 M) or $CDCl_3$ (c = 0.05 M) solutions. $^{31}P\{^1H\}$ NMR spectra of CD_2Cl_2 solution of complex **5** were obtained on a Bruker Avance 300 (operating at 121.49 MHz) in the temperature range 291–200 K. Chemical shifts (ppm) refer to the residual protic solvent peaks (5.36 ppm for ^1H and 53.45 ppm for ^{13}C), and 85% H_3PO_4 (for ^{31}P) as external standards and coupling constants are expressed in hertz (Hz), the band width at half-height ($W_{1/2}$) is given in ppm (for $^{31}P\{^1H\}$ NMR spectra). IR spectra in the region 400–4000 cm^{-1} for solid samples and in the region 920–4000 cm^{-1} for solutions were obtained on a Bruker Tensor 37 FTIR spectrometer. The samples were KBr pellets and mulls in Nujol as well as 0.01 M solutions in CD_2Cl_2 in CaF_2 cuvettes. The content of C, H, and N was determined on a Carlo Erba 1106 instrument. Melting points were determined in open capillary tubes on a Stanford Research Systems MPA120 EZ-melt automated melting point apparatus and were not corrected.

The reagents—diphenylphospine (Sigma-Aldrich), difluorobenzene (Sigma-Aldrich), sodium metal (Sigma-Aldrich), and 30% H_2O_2 (reagent grade)—were used. Salts $UO_2(NO_3)_2{\cdot}6H_2O$ (reagent grade), $Th(NO_3)_4{\cdot}5H_2O$ (pure grade), $La(NO_3)_3{\cdot}6H_2O$ (reagent grade), $Eu(NO_3)_3{\cdot}6H_2O$ (pure grade), and $Lu(NO_3)_3{\cdot}xH_2O$ (Aldrich) were used without further purification. The water content (x = 3) in commercial lutetium nitrate was determined experimentally. The following reagents were used for the preparation of solutions in the extraction study: bidistilled water, 1,2-dichloroethane (reagent grade), HNO_3 (high purity grade). Solutions for spectral and extraction studies were prepared by volumetric/gravimetric method.

4.2. Ligand synthesis

4.2.1. 1,2-Bis(diphenylphosphinyl)benzene

Sodium foil (0.37 g, 16.1 mmol) was added to a solution of 3.0 g (16.1 mmol) of diphenylphosphine in 50 mL of anhydrous THF and stirred for 4 h until complete dissolution. 1,2-Difluorobenzene (0.734 g, 0.0644 mol, 80% of the theoretical amount) was added to the resultant brown–yellow solution on cooling to −20 °C. The mixture was stirred at −20 °C for 1 h and at 20 °C for 24 h. Next, the mixture was heated for 3 h at 60 °C, cooled, and 5 mL of methanol was added to quench the excess of sodium diphenylphosphide, yellow color of solution disappeared immediately. Fifty milliliters of water was added to the solution and the mixture of solvents was removed under reduced pressure. Water (50 mL) was added to the residue, the resultant white precipitate was separated by filtration, washed with water (2 × 50 mL) and methanol (2 × 5 mL), and dried under reduced pressure to give 2.79 g (97%) of 1,2-bis (diphenylphosphinyl)benzene as a white powder, mp 184–185 °C (lit. mp 183–185 °C [16,33]). ^1H NMR (400.13 MHz, $CDCl_3$) δ: 7.40–7.32 (m, 2H, H-4,5), 7.30–7.20 (m, 20H, P-C_6H_5), 7.12–7.08 (m, 2H, H-3,6). ^{13}C NMR (100.61 MHz, $CDCl_3$) δ: 143.60 (t, $^1J_{PC}$ = $^2J_{PC}$ = 10.5, C-1,2), 136.96 (t, $^1J_{PC}$ = $^4J_{PC}$ = 2.6, *ipso*-C in Ph-P), 133.98 (t, $^2J_{PC}$ = $^3J_{PC}$ = 3.1, C-3,6), 133.77 (t, $^2J_{PC}$ = $^5J_{PC}$ = 10.0, *o*-CH in Ph-P), 128.97 (s, C-4,5), 128.23 (s, *p*-CH in Ph-P), 128.16 (t, $^3J_{PC}$ = $^6J_{PC}$ = 13.0, *m*-CH in Ph-P). $^{31}P\{^1H\}$ NMR (161.97 MHz, $CDCl_3$) δ: −14.0.

4.2.2. 1,2-Bis(diphenylphosphoryl)benzene (**L**)

Hydrogen peroxide (30% solution, 1.27 g, 11.27 mmol) was added to a solution of 2.0 g (4.48 mmol) of 1,2-bis(diphenylphosphinyl)benzene in 30 mL of chloroform with vigorous stirring. After 10 min, an exotherm was observed so that the reaction mixture warmed up to 40 °C, the mixture was stirred without cooling for 2 h. Next, 30 mL of water was added, the organic layer was separated and without drying was evaporated to dryness under reduced pressure and next dried at 80 °C for 4 h at 0.1 mmHg to give 2.14 g (quantitative) of compound **L** as a white powder, mp 137–139 °C. Spectral data corresponded to those reported in the literature [17]. ^1H NMR (400.13 MHz, $CDCl_3$) δ: 8.05–7.95 (m, 2H, H-3,6), 7.70–7.60 (m, 2H, H-4,5), 7.47 (dd, $^3J_{HH}$ = 7.8, $^3J_{PH}$ = 12.0, 8H, *o*-C<u>H</u> in Ph-P), 7.39 (t, $^3J_{HH}$ = 7.8, 4H, *p*-C<u>H</u> in Ph-P), 7.30–7.22 (m, 8H, *m*-C<u>H</u> in Ph-P). $^1H\{^{31}P\}$ NMR (400.13 MHz, $CDCl_3$) δ: 7.99 (dd, $^3J_{HH}$ = 3.8, $^3J_{HH}$ = 6.0, 2H, H-3,6), 7.64 (dd, $^3J_{HH}$ = 3.8, $^3J_{HH}$ = 6.0, 2H, H-4,5), 7.47 (d, $^3J_{HH}$ = 7.8, 8H, *o*-C<u>H</u> in Ph-P), 7.39 (t, $^3J_{HH}$ = 7.8, 4H, *p*-C<u>H</u> in Ph-P), 7.27 (t, $^3J_{HH}$ = 7.8, 8H, *m*-C<u>H</u> in Ph-P). $^{13}C\{^1H\}$ NMR (100.61 MHz, $CDCl_3$) δ: 136.10 (dd, $^1J_{PC}$ = 98.4, $^2J_{PC}$ = 7.5, C-1,2), 135.81 (t, $^2J_{PC}$ = 10.5, C-3.6), 133.01 (d, $^1J_{PC}$ = 108.5, *ipso*-C in Ph-P), 131.93 (dd, $^2J_{PC}$ = $^6J_{PC}$ = 4.0, *o*-<u>C</u>H in Ph-P), 131.23 (s, *p*-<u>C</u>H in Ph-P), 130.95 (dt, $^3J_{PC}$ = 8.5, $^4J_{PC}$ = 6.0, C-4,5), 127.71 (dd, $^3J_{PC}$ = $^5J_{PC}$ = 7.0, *m*-<u>C</u>H in Ph-P). $^{31}P\{^1H\}$ NMR (161.97 MHz, $CDCl_3$) δ: 31.4.

4.3. Synthesis of complexes of f-element nitrates

4.3.1. General procedure for the synthesis of complexes ***1*–*5***

The complexes **1**–**5**, including those suitable for X-ray diffraction analysis, were prepared according to a similar procedure, with a ratio of reagents of 1:1, and 1:2. A solution of $UO_2(NO_3)_2{\cdot}6H_2O$ or $M(NO_3)_n{\cdot}xH_2O$ (M = Th, La, Lu; n = 4, 3) in acetonitrile was added dropwise with stirring to a solution of ligand in acetonitrile. The yields were 70–90%, but no attempts were made to optimize the yield for each individual complex.

4.3.1.1. $[UO_2(\mathbf{L})(NO_3)_2]{\cdot}CH_3CN$, ***1***. A solution of 0.1147 mmol (57.6 mg) of $UO_2(NO_3)_2{\cdot}6H_2O$ in 1 mL of acetonitrile was added dropwise with stirring to a solution of 0.1147 mmol (54.8 mg) of ligand **L** in 2 mL of acetonitrile. The resultant transparent light yellow solution was stirred at ambient temperature for 1 h. One day later, a transparent light yellow crystals of $[UO_2(L)(NO_3)_2]{\cdot}CH_3CN$ formed, some of them were suitable for X-ray diffraction study. The crystals were separated by decantation, washed with cold acetonitrile and dried in vacuo (~1 Torr) at 62 °C to give 0.081 g (81%). Mp (decomp.) > 314 °C. Anal. Calcd. for $C_{30}H_{24}N_2O_{10}P_2U{\cdot}CH_3CN$: C, 42.07; H, 2.98; N, 4.60%. Found: C, 42.02; H, 2.98; N, 4.38%. IR (nujol): ν_{max}/cm^{-1} 1160vs, 1146sh (P═O), 1517vs, 1490sh (N═O), 1288 s, 1273sh (NO_2)as, 1027w (NO_2)s, 933 m, 923sh (UO_2)as. ^1H NMR (400.13 MHz, CD_2Cl_2, 0.01 M): *δ* 7.84–7.74 (~2H, m, H-4,5), 7.74–7.64 (~2H, m, H-5,6), 7,64–7.50 (~10*H*, m, C<u>H</u> in Ph), 7.49–7.35 (~7H, m, C<u>H</u> in Ph), 7.35–7.15 (~2H, v br s, C<u>H</u> in Ph). The signal of CH_3CN at 2.01 ppm is overlapped with water signal. $^{13}C\{^1H\}$ NMR (100.61 MHz, CD_2Cl_2, 0.01 M): δ (italic displays the signals of the minor component) *127.03 (*d, $^1J_{CP}$ *= 108, ipso*-C in Ph-P*)*, 127.03 (d, $^1J_{CP}$ = 110, *ipso*-C in Ph-P), 129.04 (t, $^2J_{CP}$ = 6.5, *o*-<u>C</u>H in Ph-P), *129.29–129.5 (m,* <u>C</u>H in Ph-P*)*, *132.13–132.30 (m,* <u>C</u>H in Ph-P*)*, 132.38 (t, $^3J_{CP}$ = 5.5, *m*-<u>C</u>H in Ph-P), 133.00 (dt, $^3J_{CP}$ = 6, C-4,5), *~133.78 (*br dd, $^1J_{CP}$ *= 95,* $^2J_{CP}$ *~ 7, C-1,2)*, 133.60 (s, *p*-CH in Ph-P), *133.95 (*br s, <u>C</u>H in Ph-P*)*, 134.19 (dd, $^1J_{CP}$ = 100, $^2J_{CP}$ = 7.5, C-1,2), 137.47 (t, $^2J_{CP}$ = 12.5, C-3,6); $^{31}P\{^1H\}$ NMR (161.98 MHz, CD_2Cl_2, 0.01 M): *δ* 49.0 (s, $W_{1/2}$ = 0.24), 46.4 (s, $W_{1/2}$ = 0.07), integral intensity ratio ~ 1:5.

4.3.1.2. $[UO_2(\mathbf{L})_2(NO_3)](NO_3){\cdot}CH_3CN$, ***2***. A solution of 0.1111 mmol (55.8 mg) of $UO_2(NO_3)_2{\cdot}6H_2O$ in 1.5 mL of acetonitrile was added dropwise with stirring to a solution of 0.2222 mmol (103.6 mg) of ligand **L** in 3 mL of acetonitrile. The resultant transparent light

yellow solution was stirred at ambient temperature for 4 h. One day later, the transparent solution was concentrated in vacuo (~5 Torr) up to a volume of ~1 mL. A fine-crystalline light yellow precipitate formed was separated by decantation, washed with cold acetonitrile and dried in vacuo (~1 Torr) at 62 °C to give 0.115 g (75%). Mp 296–298 °C. Anal. Calcd. for $C_{60}H_{48}N_2O_{12}P_4U{\cdot}0.5CH_3CN$: C, 51.40; H, 3.92; N, 2.46%. Found: C, 51.09; H, 3.69; N, 2.21%. IR (KBr disk, nujol): ν_{max}/cm^{-1} 1142vs, 1149sh (P═O), 1470 m (KBr disk), 1344 m, 1296 m, ~1020w, 918 m, 925sh (UO_2)as. ^1H NMR (400.13 MHz, CD_2Cl_2, 0.01 M): δ 7.82–7.72 (~4H, m, H-4,5), 7.72–7.63 (~2H, m, H-3,6), 7.64–7.53 (~14H, m, CH in Ph), 7.53–7.45 (~1H, CH in Ph), 7.45–7.35 (~10*H*, m, CH in Ph), 7.35–7.20 (~16H, v br s, CH in Ph), 7.15 (~1H, v br s, CH in Ph). 2.01 (s, CH_3CN). $^{13}C\{^1H\}$ NMR (100.61 MHz, CD_2Cl_2, 0.01 M): δ (italic displays the signals of the minor component) 127.86 (d, $^1J_{CP}$ = 112, *ipso*-C in Ph-P), *128.04 (*d, *$^1J_{CP}$ = 111, ipso*-C in Ph-P*), ~128.8 m (CH in Ph-P)*, 128.99 (t, $^2J_{CP}$ = 7, *o*-CH in Ph-P), *~132.0 br m (CH in Ph-P)*, 132.33 (t, $^3J_{CP}$ = 5, *m*-CH in Ph-P), 133.08–132.97 (m, C-4,5), 133.49 (s, *p*-CH in Ph-P), 134.04 (dd, $^1J_{CP}$ = 100, $^2J_{CP}$ = 7, C-1,2), *134.21(*dd, *$^1J_{CP}$ = 100, $^2J_{CP}$ = 8, C-1,2), 137.32 s (CH in Ph-P)*, 137.57 (t, $^2J_{CP}$ = 12.5, C-3,6); $^{31}P\{^1H\}$ NMR (161.98 MHz, CD_2Cl_2, 0.01 M): δ 46.5 (s, $W_{1/2}$ = 0.05), 46.3 (s, $W_{1/2}$ = 0.02), integral intensity ratio ~ 5:1. Transparent light yellow crystals of $[UO_2(L)_2(NO_3)_2]{\cdot}CH_3CN$, some of them suitable for X-ray diffraction study were grown from acetonitrile.

4.3.1.3. $[Th(\mathbf{L})_2(NO_3)_4]{\cdot}CH_3CN{\cdot}H_2O$, ***3***. A solution of 0.0397 g (0.0696 mmol) of $Th(NO_3)_4{\cdot}5H_2O$ in 1 mL of acetonitrile was added dropwise with stirring to a solution of 0.0666 g (0.2222 mmol) of ligand **L** in 3 mL of acetonitrile. The resultant transparent solution was stirred at ambient temperature for 4 h. After two days, the solution was evaporated to dryness under reduced pressure to give a white solid. The residue was dried in vacuo (~1 Torr) at 62 °C to give 0.085 g (85%) of the title compound. Mp 178–180 °C. Anal. Calcd. for $C_{60}H_{48}N_4O_{16}P_4Th{\cdot}CH_3CN{\cdot}H_2O$: C, 49.78; H, 3.57; N, 4.68%. Found: C, 49.54; H, 3.33; N, 4.11%. IR (nujol): ν_{max}/cm^{-1} 1136 s (P═O), 1512 m (N═O), 1288 m (NO_2)as, 1023w (NO_2)s. ^1H NMR (500.13 MHz, CD_2Cl_2, 0.01 M): δ 7.80–7.77 (4H, m, H-4,5), 7.49 (8H, dt, *p*-CH in Ph-P), 7.46–7.42 (4H, m, H-3,6), 7.40–7.36 (16H, m, CH in Ph), 7.28–7.24 (16H, m, CH in Ph). 2.01 (s, CH_3CN). $^{13}C\{^1H\}$ NMR (125.75 MHz, CD_2Cl_2, 0.01 M): δ 126.43 (d, $^1J_{CP}$ = 112.5, *ipso*-C in Ph-P), 129.27–129.10 (m, CH in Ph), 132.26–132.10 (m, CH in Ph), 133.22–133.04 (m, C-4,5), 133.21 (dd, $^1J_{CP}$ = 101.2, $^2J_{CP}$ = 7.5, C-1,2), 133.87 (s, *p*-CH in Ph-P), 137.84 (t, $^2J_{CP}$ = 12.5, C-3,6). $^{31}P\{^1H\}$ NMR (202.46 MHz, CD_2Cl_2, 0.01 M): δ 44.9 (s, $W_{1/2}$ = 0.01).

4.3.1.4. $[La(\mathbf{L})_2(NO_3)_3]{\cdot}0.5CH_3CN{\cdot}1.5H_2O$, ***4***. This compound was synthesized according to the general method similar to the preparation of complex **2** from 0.0758 mmol (32.8 mg) of $La(NO_3)_3{\cdot}6H_2O$ and 0.1517 mmol (72.6 mg) of **L**. The mixture was concentrated in vacuo (~5 Torr) to a volume of ~0.7 mL. The fine-crystalline white precipitate formed was filtered, washed by cold acetonitrile, and dried in vacuo (~1 Torr) at 62 °C to give 0.069 g (70.1%) of complex **4**. Mp 218–221 °C. *Anal.* Calcd. for $C_{60}H_{48}LaN_3O_{13}P_4{\cdot}0.5CH_3CN{\cdot}1.5H_2O$: C, 55.11; H, 3.98; N, 3.69%. Found: C, 55.17; H, 4.04; N, 3.70%. IR (nujol): ν_{max}/cm^{-1} 1178vs (P═O), 1317 s, 1295sh, 1936w, 1031sh. ^1H NMR (400.13 MHz, CD_2Cl_2, 0.01 M): δ 7.60–7.52 (~4H, m, H-4,5), 7.5 2–7.40 (~15H, m, CH in Ph), 7.40–7.20 (~10*H*, m, CH in Ph), 7.25–7.0 5 (~14H, CH in Ph). 2.01 (s, CH_3CN). No signal of H-3,6 nuclei was observed. $^{13}C\{^1H\}$ NMR (100.61 MHz, CD_2Cl_2, 0.01 M): δ 128.52–128.36 (m, CH in Ph), 129.44 (d, $^1J_{CP}$ = 110, *ipso*-C in Ph-P), 131.61–131.39 (m, C-4,5), 132.23–132.24 (m, CH in Ph), 132.28 (s, CH in Ph), 135.84 (dd, $^1J_{CP}$ = 100, $^2J_{CP}$ = 8, C-1,2), 136.83 (t, $^2J_{CP}$ = 12, C-3,6). $^{31}P\{^1H\}$ NMR (161.98 MHz, CD_2Cl_2, 0.01 M): δ 35.4 (s, $W_{1/2}$ = 0.05).

4.3.1.5. $[Lu(\mathbf{L})_2(NO_3)_3]{\cdot}2CH_3CN$, ***5***. This compound was synthesized according to the general method similar to preparation of complex **2**, from 0.0758 mmol (31.5 mg) of $Lu(NO_3)_3{\cdot}3H_2O$ and 0.1517 mmol (72.6 mg) of **L**. The mixture was concentrated in vacuo (~5 Torr) to a volume of ~ 0.7 mL. Transparent crystals of **5** formed, some of them were suitable for X-ray diffraction study. The crystals were separated by decantation, washed with cold acetonitrile, and dried in vacuo (~1 Torr) at 62 °C to give 0.065 g (65%) of complex **5**. Mp 181–183 °C. *Anal.* Calcd. for $C_{60}H_{48}LuN_3O_{13}P_4{\cdot}0.5CH_3CN{\cdot}0.5H_2O$: C, 54.37; H, 3.78; N, 3.64. Found: C, 54.39; H, 3.97; N, 3.84%. IR (nujol): ν_{max}/cm^{-1} 1167 s, 1145 s (P═O), ~1500 m, 1340 m, 1305 m, 1027w, 2249w (C≡N), 3390w (H_2O). H NMR (400.13 MHz, CD_2Cl_2, 0.01 M): δ 7.82–7.92 (4H, v br s, H-4,5), 7.55–7.49 (8H, m, *p*-CH in Ph-P), 7.50–7.38 (4H, br m, H-3,6), 7.29–7.20 (32H, br m, CH in Ph),. 2.01 (s, CH_3CN). $^{13}C\{^1H\}$ NMR (100.61 MHz, CD_2Cl_2, 0.01 M): δ 127.29 (d, $^1J_{CP}$ = 112, *ipso*-C in Ph-P), 129.04 (t, $^2J_{CP}$ = 6.5, *o*-CH in Ph-P), 131.88 (t. $^3J_{CP}$ = 5.5, *m*-CH in Ph-P), 133.4–133.0 (m, C-4,5), 133.56 (s, *p*-CH in Ph-P), 134.22 (dd, $^1J_{CP}$ = 100, $^2J_{CP}$ = 7, C-1,2), 137.86 (t, $^2J_{CP}$ = 12, C-3,6). $^{31}P\{^1H\}$ NMR (161.98 MHz, CD_2Cl_2, 0.01 M): δ 41.9 (s, $W_{1/2}$ = 0.05).

4.3.2. Procedure for the preparation of model solution with metal: ligand ratios of 1:3

To prepare solution with metal:ligand molar ratio of 1:3, a calculated amount of ligand **L** was added to a 0.01 M solution of complex **4** in CD_3CN.

4.4. X-ray crystallography

Single crystals of **1**, **5** were obtained from reaction mixture, single crystals of **2** were grown from MeCN. The intensities of reflections were measured with a Bruker Apex II (**2**) or a Bruker D8 Quest (**1**, **5**) CCD diffractometer using graphite monochromated MoKα radiation (λ = 0.71073 Å) at 120 and 296 K, respectively. The structures were solved by the SHELXT method [34] and refined by full-matrix least squares against F^2. Non-hydrogen atoms were refined anisotropically. The positions of all hydrogen atoms were calculated, and were included in the refinement by the riding model with U_{iso}(H) = 1.5U_{eq}(X) for methyl groups, and 1.2U_{eq}(C) for the other atoms. All calculations were made using the SHELXL2014 [35] and OLEX2 [36] program packages. Crystal parameters and refinement details are listed in Table 5. CCDC 2039977–2039979 for complexes **1**, **2**, **5** contain the supplementary crystallographic data for these compounds.

4.5. Computational details

Geometry optimization of uranyl complex $[UO_2\mathbf{L}(NO_3)_2]$ and cation of bisligand complex $[UO_2\mathbf{L}_2(NO_3)]^+$ was done with GAUSSIAN 09 [37] software suite on DFT level of theory. The hybrid PBE0 [38] functional and Stuttgart MWB60 basis set [39] for U atom and 6-311+G** [40] basis set for other atoms were utilized. Topological analysis of electron density according to Bader's "Atoms in Molecules" theory (AIM) [41] was performed in AIMAll [42] program, in which connection ECP MWB60 basis set for U atom was changed to all-electron basis set [43]. Interaction energies of π-stacking and C—H…π

Table 5
Crystallographic data and refinement parameters for $[UO_2\mathbf{L}(NO_3)_2]$ MeCN (**1**), $[UO_2\mathbf{L}_2(NO_3)](NO_3)\cdot$MeCN (**2**), and $[Lu\mathbf{L}_2(NO_3)_2](NO_3)\cdot$2MeCN (**5**).

	1	**2**	**5**
Empirical formula	$C_{32}H_{27}N_3O_{10}P_2U$	$C_{62}H_{50}N_3O_{12}P_4U$	$C_{64}H_{48}LuN_5O_{13}P_4$
Fw	913.53	1390.96	1393.92
Color, habit	Yellow, prism	Yellow, prism	Colorless, prism
Crystal size (mm)	0.46 × 0.20 × 0.13	0.38 × 0.12 × 0.12	0.25 × 0.21 × 0.11
Crystal system	Monoclinic	Monoclinic	Monoclinic
Space group	$P2_1/n$	$C2/c$	$C2/c$
a (Å)	9.5720(1)	31.167(3)	16.4529(3)
b (Å)	28.5901(4)	18.9090(15)	15.4128(3)
c (Å)	12.8343(2)	21.5536(17)	25.0928(4)
β (°)	91.1199(6)	107.863(2)	96.5138(7)
V (Å^3)	3511.62(8)	12089.9(17)	6322.1(2)
Z	4	8	4
μ (cm^{-1})	4.771	2.854	1.729
D_{calc} (g cm^{-3})	1.728	1.528	1.385
F(000)	1768	5528	2808
No. of measured, independent and observed [$I > 2\sigma(I)$] reflections	64634, 13986, 10.,567	82423, 18484, 11.,941	62829, 13920, 11.,348
R_{int}	0.0426	0.0924	0.0455
$R[F^2 > 2\sigma(F^2)]$, $wR(F^2)$, S	0.0335, 0.0694, 1.1	0.0577, 0.1615, 1.0	0.0409, 0.1082, 1.0
$\Delta\rho_{max}$, $\Delta\rho_{min}$ (e Å^{-3})	1.17, −1.12	2.74, −2.44	2.00, −0.94

contacts were estimated with Espinosa's correlation scheme $E_{cont} = -1/2V(\mathbf{r})$ [44].

4.6. Extraction of f-elements

1,2-Dichloroethane (DCE) of reagent grade was used without additional purification as the organic solvent. Solutions of extractants were prepared from accurately weighed samples. The initial aqueous solutions of lanthanides(III), U(VI), and Th(IV) were prepared by dissolving the respective nitrates in water followed by the addition of HNO_3. The initial concentrations of metal ions were $2 \cdot 10^{-6}$ M, the concentration of HNO_3 was 2 M. The extraction experiments were performed in test tubes equipped sealing plugs at room temperature and 1:1 vol ratio of organic and aqueous phases. The phases were contacted in a rotary mixer at rate of 60 rpm for 1 h, this time being sufficient to reach constant values of the distribution ratio (D_M).

The concentration of Ln(III), U(VI) and Th(IV) in the initial and equilibrated aqueous solutions was determined by mass spectrometry with inductively coupled plasma ionization of samples (ICP-MS), using a Thermo Elemental X-7 mass spectrometer according to a published method [45]. The content of elements in the organic phase was obtained from the material balance. The distribution ratios for the elements were calculated as ratios of the equilibrium concentration in the organic and aqueous phases ($D_M = [M_{org}]/[M_{aq}]$). Triple experiments showed that the reproducibility of the D was generally within 5%.

CRediT authorship contribution statement

Anna G. Matveeva: Conceptualization, Methodology, Writing - review & editing. **Oleg I. Artyushin:** Data curation. **Margarita P. Pasechnik:** Data curation. **Adam I. Stash:** Data curation. **Anna V. Vologzhanina:** Data curation, Visualization. **Sergey V. Matveev:** Data curation, Visualization. **Ivan A. Godovikov:** Data curation. **Rinat R. Aysin:** Data curation. **Aleksandra A. Moiseeva:** Data curation. **Alexander N. Turanov:** Data curation. **Vasilii K. Karandashev:** Data curation. **Valery K. Brel:** Supervision.

Declaration of Competing Interest

The authors declare that they have no known competing financial interests or personal relationships that could have appeared to influence the work reported in this paper.

Acknowledgement

This work was financially supported by the Russian Science Foundation (project no. 20–13–00329). Spectral studies were carried out with the financial support from the Ministry of Science and Higher Education of the Russian Federation using the equipment of the Center for Molecular Structure Studies, INEOS RAS.

Appendix A. Supplementary data

CCDC 2039977 (**1**), 2039978 (**2**) and 2039979 (**5**) contain the supplementary crystallographic data for this paper. These data can be obtained free of charge via http://www.ccdc.cam.ac.uk/conts/retrieving.html, or from the Cambridge Crystallographic Data Centre, 12 Union Road, Cambridge CB2 1EZ, UK; fax: (+44) 1223-336-033; or e-mail: deposit@ccdc.cam.ac.uk. Supplementary data to this article can be found online at https://doi.org/10.1016/j.poly.2021.115085.

References

[1] S.A. Cotton, Lanthanide and Actinide Chemistry, John Wiley, Chichester, 2006.
[2] S.A. Cotton, in: Comprehensive Coordination Chemistry II, 4, Elsevier, Oxford, 2004, p. 93.
[3] S.A. Cotton, P.R. Raithby, Coord. Chem. Rev. 340 (2017) 220.
[4] A.W.G. Platt, Coord. Chem. Rev. 340 (2017) 62.
[5] A. Leoncini, J. Huskens, W. Verboom, Chem. Soc. Rev. 46 (2017) 7229.
[6] M.Y. Alyapyshev, V.A. Babain, Y.A. Ustynyuk, Russ. Chem. Rev. 85 (2016) 943.
[7] Y. Lu, H. Wei, Z. Zhang, Y. Li, G. Wu, W. Liao, Hydrometallurgy 163 (2016) 192.
[8] M.I. Kabachnik, Heteroatom. Chem. 2 (1991) 1.
[9] M.I. Kabachnik, Y.M. Polikarpov, Russ. J. Gen. Chem. 58 (1988) 1937 (in Russian).
[10] H.H. Dam, D.N. Reinhoudt, W. Verboom, Chem. Soc. Rev. 36 (2007) 367.
[11] B.W. McCann, N. De Silva, T.L. Windus, M.S. Gordon, B.A. Moyer, V.S. Bryantsev, B.P. Hay, Inorg. Chem. 55 (2016) 5787.
[12] F. de María Ramírez, S. Varbanov, J. Padilla, J.-C. G. Bünzli, J. Phys. Chem. B, 112 (2008) 10976
[13] A.E.V. Gorden, M.A. DeVore, B.A. Maynard, Inorg. Chem. 52 (2013) 3445.
[14] M.B. Jones, A.J. Gaunt, Chem. Rev. 113 (2013) 1137.
[15] A.N. Turanov, V.K. Karandashev, O.I. Artyushin, V.K. Brel, Solvent Extr. Ion Exch. 38 (2020) 166.
[16] H.C.E. McFarlane, W. McFarlane, Polyhedron 2 (1983) 303.
[17] M. Stankevič, A. Włodarczyk, Tetrahedron 69 (2013) 73.
[18] R.D. Bannister, W. Levason, G. Reid, W. Zhang, Polyhedron 133 (2017) 264.
[19] K. Nakamura, Y. Hasegawa, H. Kawai, N. Yasuda, Y. Wada, S. Yanagida, J. Alloys Compd. 408–412 (2006) 771.
[20] M.F. Davis, W. Levason, R. Ratnani, G. Reid, M. Webster, New J. Chem. 30 (2006) 782.
[21] M.B. Hursthouse, W. Levason, R. Ratnani, G. Reid, Polyhedron 23 (2004) 1915.
[22] M.F. Davis, W. Levason, G. Reid, M. Webster, Polyhedron 25 (2006) 930.
[23] A.R.J. Genge, W. Levason, G. Reid, Inorg. Chim. Acta 288 (1999) 142.
[24] N.J. Hill, W. Levason, M.C. Popham, G. Reid, M. Webster, Polyhedron 21 (2002) 445.

[25] M.B. Hursthouse, W. Levason, R. Ratnani, G. Reid, H. Stainer, M. Webster, Polyhedron 24 (2005) 121.
[26] R.D. Bannister, W. Levason, M.E. Light, G. Reid, W. Zhang, Polyhedron 167 (2019) 1.
[27] K. Nakamoto, Infrared and Raman Spectra of Inorganic and Coordination Compounds, J. Wiley & Sons Inc., Hoboken, 2009.
[28] A.G. Matveeva, A.S. Peregudov, E.I. Matrosov, Z.A. Starikova, S.V. Matveev, E.E. Nifant'ev, Inorg. Chim. Acta 362 (2009) 3607.
[29] A.N. Turanov, V.K. Karandashev, A.V. Kharitonov, Z.V. Safronova, A.N. Yarkevich, Radiochemistry 42 (2000) 349 [in Russian].
[30] J. Overgaard, M.P. Waller, R. Piltz, J.A. Platts, P. Emseis, P. Leverett, P.A. Williams, D.E. Hibbs, J. Phys. Chem. A 111 (2007) 10123.
[31] A.G. Matveeva, A.V. Vologzhanina, E.I. Goryunov, R.R. Aysin, M.P. Pasechnik, S. V. Matveev, I.A. Godovikov, A.M. Safiulina, V.K. Brel, Dalton Trans. 45 (2016) 5162.
[32] W.L.F. Armarego, C.L.L. Chai, Purification of Laboratory Chemicals, sixth ed., Elsevier, Amsterdam, Boston, 2009.
[33] H. Christina, E. McFarlane, W. McFarlane, Polyhedron 7 (1988) 1875.
[34] G.M. Sheldrick, Acta Cryst. A71 (2015) 3.
[35] G.M. Sheldrick, Acta Cryst. C71 (2015) 3.
[36] O.V. Dolomanov, L.J. Bourhis, R.J. Gildea, J.A.K. Howard, H. Puschmann, J. Appl. Cryst. 42 (2009) 339.
[37] Gaussian 09, Revision D.01, M.J. Frisch, G.W. Trucks, H.B. Schlegel, G.E. Scuseria, M.A. Robb, J.R. Cheeseman, G. Scalmani, V. Barone, B. Mennucci, G.A. Petersson, H. Nakatsuji, M. Caricato, X. Li, H.P. Hratchian, A.F. Izmaylov, J. Bloino, G. Zheng, J.L. Sonnenberg, M. Hada, M. Ehara, K. Toyota, R. Fukuda, J. Hasegawa, M. Ishida, T. Nakajima, Y. Honda, O. Kitao, H. Nakai, T. Vreven, J.A. Montgomery, Jr., J.E. Peralta, F. Ogliaro, M. Bearpark, J.J. Heyd, E. Brothers, K.N. Kudin, V.N. Staroverov, T. Keith, R. Kobayashi, J. Normand, K. Raghavachari, A. Rendell, J.C. Burant, S.S. Iyengar, J. Tomasi, M. Cossi, N. Rega, J.M. Millam, M. Klene, J.E. Knox, J.B. Cross, V. Bakken, C. Adamo, J. Jaramillo, R. Gomperts, R.E. Stratmann, O. Yazyev, A.J. Austin, R. Cammi, C. Pomelli, J.W. Ochterski, R.L. Martin, K. Morokuma, V.G. Zakrzewski, G.A. Voth, P. Salvador, J.J. Dannenberg, S. Dapprich, A.D. Daniels, O. Farkas, J.B. Foresman, J.V. Ortiz, J. Cioslowski, D.J. Fox, Gaussian, Inc., Wallingford CT, 2013.
[38] C. Adamo, V. Barone, J. Chem. Phys. 110 (1999) 6158.
[39] (a) W. Kuechle, M. Dolg, H. Stoll, H. Preuss, J. Chem. Phys. 100 (1994) 7535; (b) X. Cao, M. Dolg, H. Stoll, J. Chem. Phys. 118 (2003) 487; (c) X. Cao, M. Dolg, J. Molec. Struct. (Theochem) 673 (2004) 203.
[40] [(a) R. Krishnan, J.S. Binkley, R. Seeger, J.A. Pople, J. Chem. Phys. 72 (1980) 650; (b) A.D. McLean, G.S. Chandler, J. Chem. Phys. 72 (1980).
[41] R.F.W. Bader, Atoms in Molecules. A Quantum Theory, Clarendron Press, Oxford, 1990.
[42] T.A Keith,. AIMAll (Ver. 19.10.12); TK Gristmill Software: , 2019 (aim. tkgristmill.com).
[43] (a) D.A. Pantazis, F. Neese, J. Chem. Theory Comput. 5 (2009) 2229; (b) D.A. Pantazis, F. Neese, J. Chem. Theory Comput. 7 (2011) 677.
[44] (a) E. Espinosa, E. Molins, C. Lecomte, Chem. Phys. Lett. 285 (1998) 170; (b) E. Espinosa, I. Alkorta, I. Rozas, J. Elguero, E. Molins, Chem. Phys. Lett. 336 (2001) 457.
[45] A.N. Turanov, V.K. Karandasshev, V.E. Baulin, Solvent Extr, Ion Exch. 14 (1996) 227.